A Snapshot of Suspended Sediment Concentrations and Fluxes using Optical and Acoustic Velocity Profilers,The Stour Estuary, Suffolk, UK.

Report for: ARGUS GESELLSCHAFT FUER UMWELTMESSTECHNIK MBH, 3rd March 2003

M.B. Gilpin,
Department of Earth & Environmental Sciences, The University of Greenwich at Medway, Chatham Maritime, Kent ME4 4TB

Abstract

Measurements of the spatial and temporal change in suspended sediment concentration (SSC), using an Argus Surface Meter IV (ASM), and current velocity profiles, using a bottom-mounted acoustic Doppler profiler (ADCP), were obtained over one tidal cycle. The aim of the experiment was to determine whether the ASM, primarily designed to detect bed-level erosion and scour, could operate as a multi-sensor optical backscatter device (OBS). Unlike a single sensor OBS, the instrument has an array of sensors with a measuring profile of approximately 1metre. During the tidal cycle the ASM successfully detected a decrease in concentration due to particle settling during the lowest current velocities and re-suspension of particles during peak current flow. Concentration data correlated well with data obtained from a LISST suspended sediment sensor (LISST) and gravimetrically determined samples and thus operated favourably as a multi-sensor OBS, indicative of a successful calibration.

Contents

1. Introduction

1.1 Aims and Objectives

This report presents the results of an Argus Surface Meter IV (ASM) laboratory calibration and a field experiment carried out at Harwich on the Stour Estuary, Suffolk, England (figure 1), on the 28th May 2002. The aim was to determine whether this instrument could operate as a multi-sensor OBS. The objective was to match SSC profiles to current velocity profiles, for the determination of sediment fluxes, by deploying the ASM with an Acoustic Doppler profiler (figure 2).

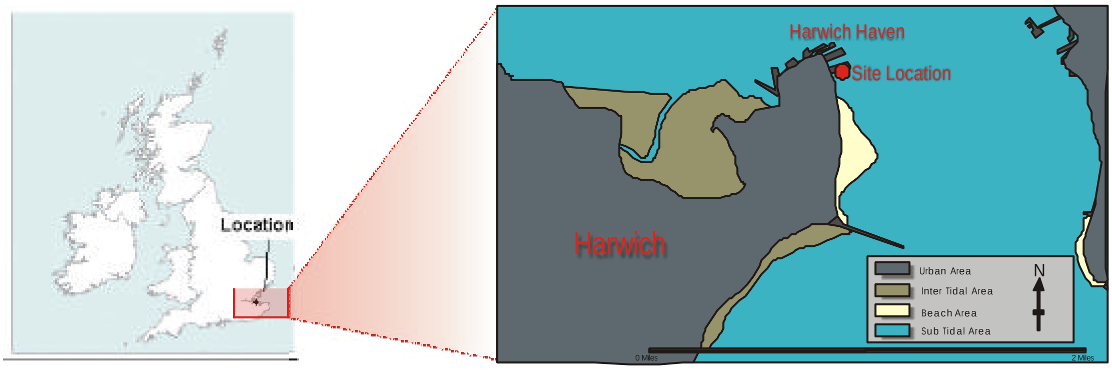

Figure 1: Location of the Harwich Haven Port Authority, on the Stour Estuary, Suffolk, England.

Figure 2: Photo of the deployment site, showing the location of the ASM and ADCP.

The calibration technique was designed to increase the sensitivity of the ASM to particulate reflectance at much lower concentrations than the instrument was originally designed for. The ASM was primarily developed for high-resolution measurements at the bottom of moving water to provide a clear discrimination of the dynamic boundary layer between the seabed and the suspension area above. The SSC's derived from calibrated data were compared with measured concentrations determined gravimetrically from filtered samples and to data derived from a LISST suspended sediment sensor to assess the ASM's performance.

1.2 Optical Backscatter Sensors

The introduction of optical backscatter sensors have increased suspended sediment sampling densities and significantly improved our understanding of SSC dynamics in the marine environment . These instruments respond directly to SSC's and thus may be used to identify process-driven variations in water turbidity, and to estimate residual sediment transport fluxes in estuarine channels. The heart of an OBS monitor is the optical sensor for measuring suspended solids concentrations by detecting infrared radiation scattered from suspended matter. The sensors can be calibrated to detect suspended solids directly, but the response depends on the size, composition and shape of suspended particles. For this reason, OBS sensors must be calibrated with suspended solids from the waters to be monitored.

The ASM IV records the reflections and the dynamic parameters that are created in the water column by solid particles moving in a multiphase current. Activation of the data logger and the power supply of the sensors, as well as the transmission of the signals, are controlled from a battery powered central unit in the head of the instrument. The sealed in unit consists of a microprocessor, a data memory, additional sensors (temperature, pressure and tilt gauges) and the energy supply. Incoming data is processed by the microprocessor and stored in the memory.

The instrument operates with backscatter infrared sensors that are embedded in intervals in a solid pile made of stainless steel (Figure 3). The sensors are spaced at 10 mm, 96 sensors in total, which gives a measuring profile of approximately 1m. Each sensor consists of an infrared transmitter and detector. The backscatter/reflection samples taken have a volume of approx. 0.5 cm^3 at a distance between 5 and 10 mm in front of the sensor. Optical filters and a high current transmitting light source prevent interference by other light sources. This makes the instrument suitable for locations like tidal areas with dry periods. The reflectivity of infrared light does not depend on the size particles encountered but on their reflection or absorption properties, i.e. white has a high reflectivity and black has a very low reflectivity even if the material is the same. This is why each calibration has to be site/sediment specific.

ASM-IV CONSTRUCTION

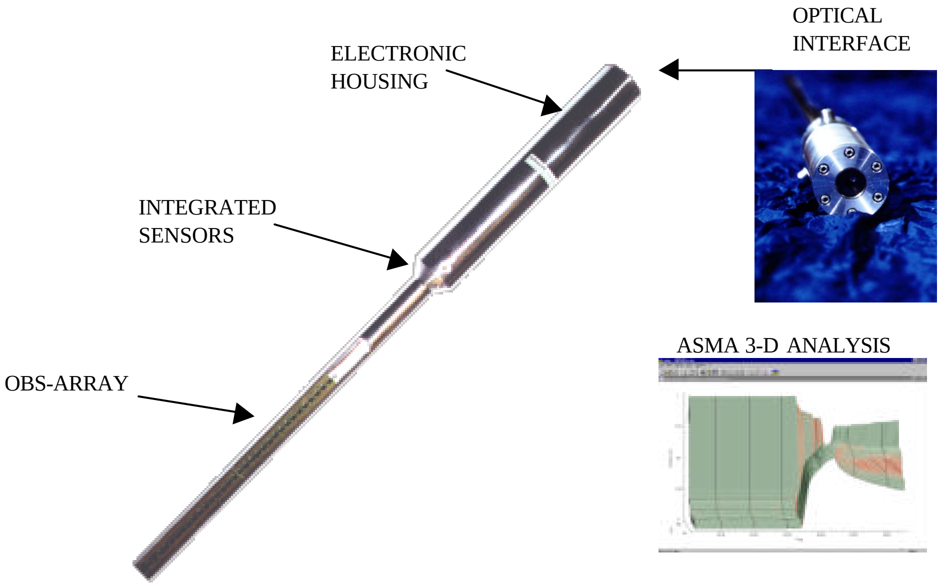

Figure 3: Argus Surface Meter ASM-IV construction.

2. Calibration

The aim of a calibration is to set the maximum and minimum response ranges of the sensors to match the highest/lowest output voltage (expressed as reflectivity counts for the ASM IV) expected from the OBS in the field with the input span of the instrument's data logger. Undesirable results will be obtained if the gain is not correctly adjusted; when the gain is too high, data will be lost because the sensors output is limited by the supply voltage and will saturate before peaks in sediment concentration are detected. If the gain is too low, the full resolution of the data will not be utilized.

A layer of bed sediment was extracted, at a depth of 0.5cm, at low tide from the deployment site for the calibration. A sub sample of the sediment was sieved to obtain particle size distribution information (Figure 4).

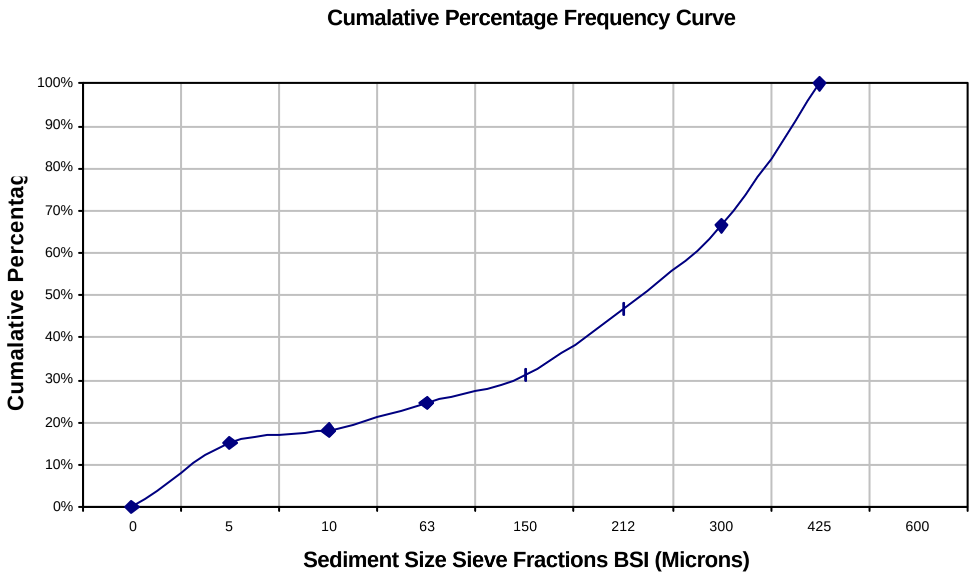

Figure 4: Particle size distribution curve for the calibration sediment sample. Bed sediment at the deployment site consists mainly of fine sands and clay with a small percentage of silts.

To set the minimum response range, the instrument was inserted into a calibration tank with the whole OBS array submerged in clear water. The water was then pumped around the tank and the ASM activated. The reflectivity counts recorded (approximately 50 to 60) were logged and automatically adjusted to the minimum gain of the instrument (0 counts). To set the maximum response range bed sediment taken from the survey site was added to the tank until the reflectivity increased until approximately 600 counts (the approximate maximum concentration of sediment expected at the deployment site) logged and automatically adjusted to the maximum gain of the instrument (4095 counts).

Whilst the pump was still running the probe was set to record in real time. A calibration curve is then computed by diluting the water/sediment mixture to seven different concentrations covering the range from maximum to minimum (figure 5). At each dilution time-step bottle samples were taken from taps along the tank and the time of each sample taken was recorded. Each tap corresponds to a 32-sensor block of the 96-sensor probe. The bottle samples were then filtered gravimetrically to provide a comparison of concentrations that corresponded to the instrument reflectivity counts recorded at the same time step. These are then plotted as X (reflectivity) and Y (concentration) data points on a scatter plot and a second order polynomial trend line fitted and the resultant equations extracted. Sediment concentration is the dry weight of sediment divided by the volume of sample in litres (expressed as mg l^{-1}).

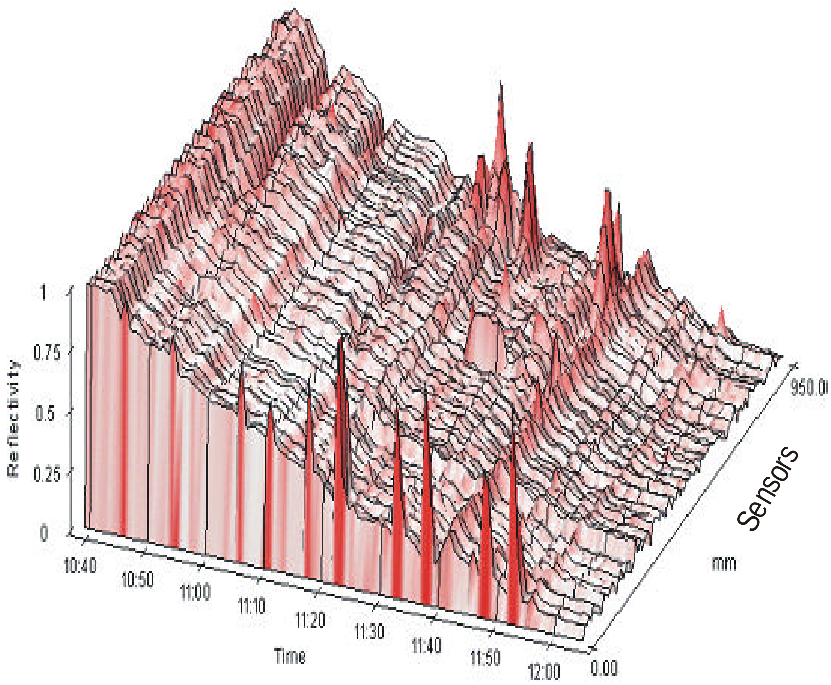

Figure 5: The calibration run, each reduction in reflectivity corresponds with the diluting of the tank, at each dilution time step a bottle sample was taken.

3. Results and Discussion

3.1 Suspended Sediment Particle Size

Figure 6 compares the particle sizes in suspension during the deployment period from two particle size analysis methods. A LISST-25 in-situ laser sizer was deployed at 0.12m above the bed and pumped bottle samples taken every fifteen minutes at 0.5m above the bed. The LISST data shows there was a range of fine sands to coarse silts in suspension between 09:00hrs and 10:15hrs, coarse sands from 10:15hrs to 13:00hrs and only coarse silts between 13:00hrs and 16:00hrs. The pumped samples show a range of clays to fine silts throughout the deployment period. The pumped samples where sized using a Malvern Laser Sizer; a method that requires the de-aggregation of any aggregates present in a sample. Therefore the contrary results between the two sizing methods suggest that the LISST has detected suspended mud flocculation (flocs). This has implications for the calibration technique, inasmuch as:

- Does the calibration tank break up any flocs in the bed sediment used for the calibration?
- If so, was the ASM calibrated with sediment that includes the full range of particle sizes expected in suspension during the deployment?
- If not, was the ASM calibrated with the presence of flocs in the sediment and was it the size of the flocs rather than their colour that was the major factor affecting the reflectivity recorded?

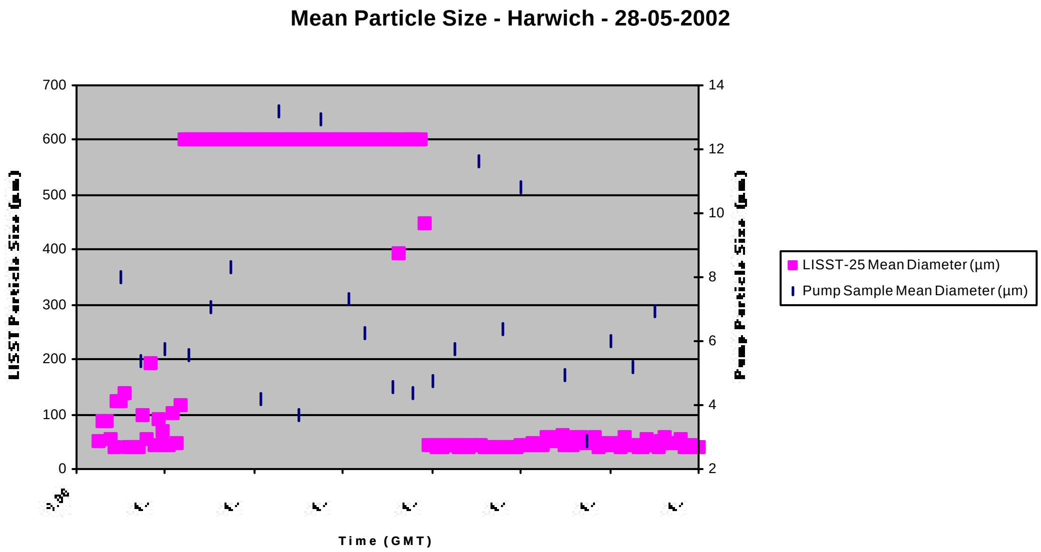

Figure 6: Comparison of particle size analysis using a LISST-25 and pumped bottles samples. The LISST data shows there was a range of fine sands to coarse silts whereas the pumped samples show a range of clays to fine silts.

3.2 ASM graphic representations of recorded reflectivity and variance from the deployment.

The ASM was deployed so that sensors 96 to 75 were fully submerged within the bed itself; this corresponded to a measuring profile of 0.75m. The probe was set to start recording at 08:00 GMT; the tide began to cover the first exposed sensor (sensor 75) at approximately 08:05 and all the sensors were covered by 09:05. The tide was observed to change from flood to ebb at approximately 12:55. There was a strong wind through most of the day and a strong current noticed flowing counter to the prevailing ebb tidal current.

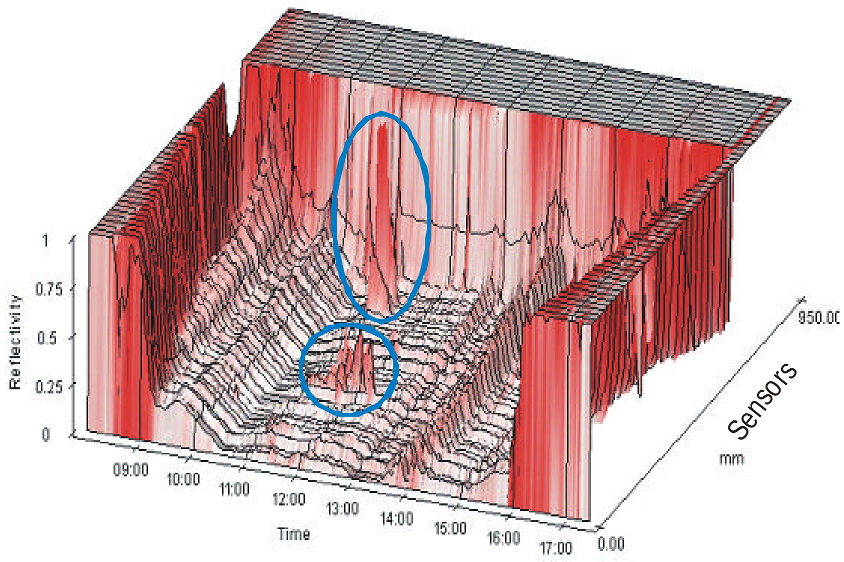

Figure 7: 3D view showing the results of the deployment, where height represents reflectivity and colour represents the variance in the reflectivity (a proxy for SSC) measurements.

Notice the increase in reflectivity recorded at the peak flood and ebb periods (approx 09:30 and 14:00 respectively) in figure 7. Increase reflectivity circled in blue may correspond to contamination of the data by debris (weeds/reeds). The red colouring on the graph represents the variance of the reflectivity recorded from ten single measurements within a sampling cycle of every fifty seconds. The dark red areas of the graph represent a greater variation between the ten measurements within this temporal scale, which represents a greater degree of variation in sediment reflectivity.

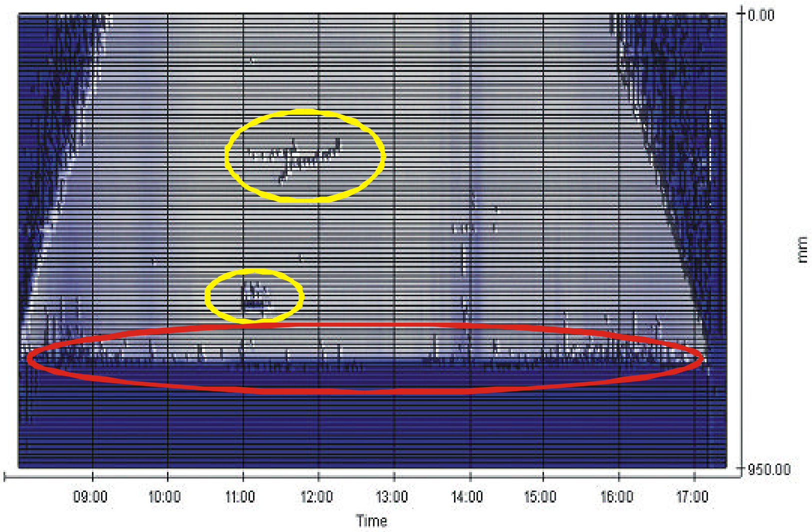

Figure 8: 2D view showing the results of the deployment, where height represents variance and colour represents the reflectivity.

Figure 8 shows the same information as figure 7 but in 2D and orientated 180^0 on the Y plane and 90^0 on the X plane. The two dark blue areas at either side of the graph show the times of maximum reflectivity recorded when the sensors were exposed to open air. The light blue colouring within the yellow area represents the increases in reflectivity recorded at the peak flood and ebb periods (approx 09:30 and 14:00 respectively). The dark blue along the bottom indicates maximum reflectivity recorded from within the bed sediments. At this scale it is not possible to detect a change in reflectivity along the water/bed interface. However, the reflectivity variance, shown by clusters of peaks and troughs along the surface (circled red), correspond well with the ebb and flood periods of increase reflectivity. This may indicate that the same processes that are increasing suspended sediment concentrations, i.e. increase current velocities at peak flow periods, are entraining the bed sediments. This may also imply that the sediments in suspension originate from the bed and are derived locally. The effect of the mud within the bed will increase the variation in the reflectivity measurements due to the varying response produced by a sand and mud mixture. The two bursts of increase reflectivity circled in blue in figure 7 are circled yellow in this graph.

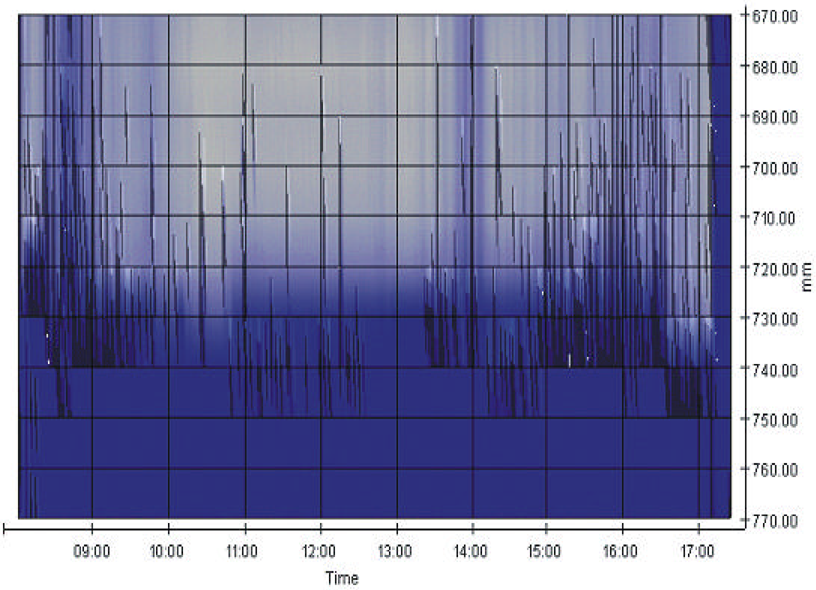

Figure 9: 2D graphic of the sediment/water interface, where height represents variance and colour represents reflectivity.

Figure 9 shows a more detailed plot of the processes observed at the sediment/water interface circled red in figure 8. The yellow colour indicates the water column with low sediment concentrations and the black colour indicates the areas of the bed with high concentrations. The changing dynamics of the reflectivity represented by the black and blue areas indicates increases and decreases of reflectivity within the bed. There is a possibility that this is indicative of a fluid mud layer at this location of approximately 3 cm thick. At 10:30 and 13:00 hours the tidal current changes to slack water and these dynamic processes stop.

3.3 Graphic representations of the recorded reflectivity converted to concentrations

Notice the increase in suspended load recorded at the peak flood and ebb periods, approx 5000 (09:30) and 20000 (14:00) respectively in figure 10. The dark blue area along the bottom of the graph indicates the maximum concentrations recorded from the bed sediment suspension. At 10:30 and 13:00 hours the tidal current changes to slack water and these dynamic processes stop. Suspended sediment concentrations range from 160mg/l to 500mg/l, indicative of high-concentration mud suspension (HCMS). An important feature of HCMS is its interaction with a turbulent flow field.

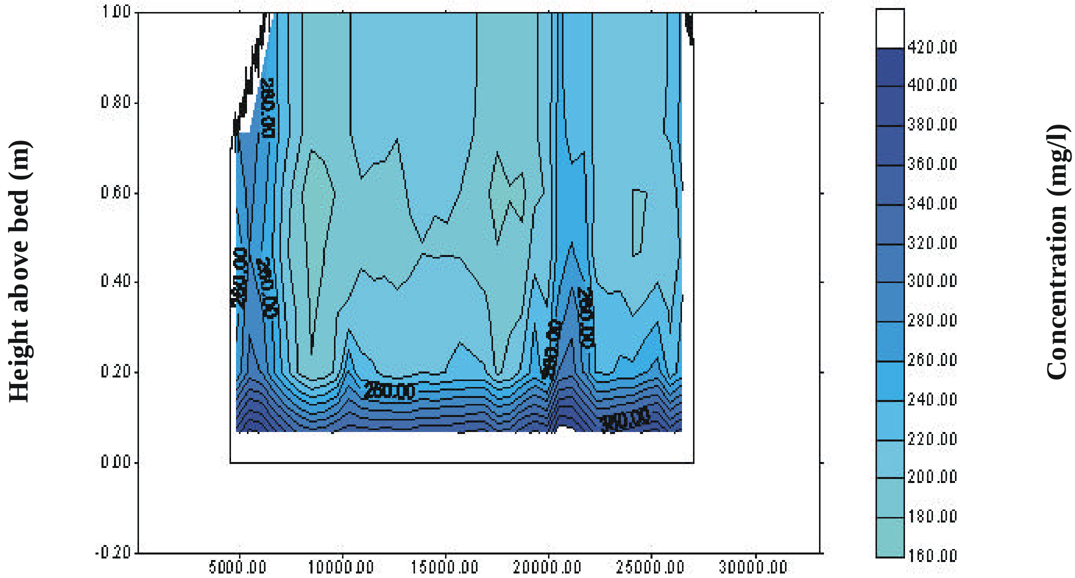

Figure 10: Graph of reflectivity converted to concentrations.

The suspended sediment concentration profile for the peak flood period is more uniform throughout the water column than for the peak ebb period (figure 11). This corresponds to the shallower gradient of the floodtide compared to the steeper gradient of the ebb tide (figure 14). There are higher sediment concentrations in suspension at the bed level during the peak ebb period (figure 13) than the peak flood period. This corresponds to the steeper gradient of the ebb tide and thus higher current velocities producing more suspended sediment (figure 14). The slack water concentration profile exhibits a greater range of sediment concentrations (figure 12), suggesting a sediment-settling period.

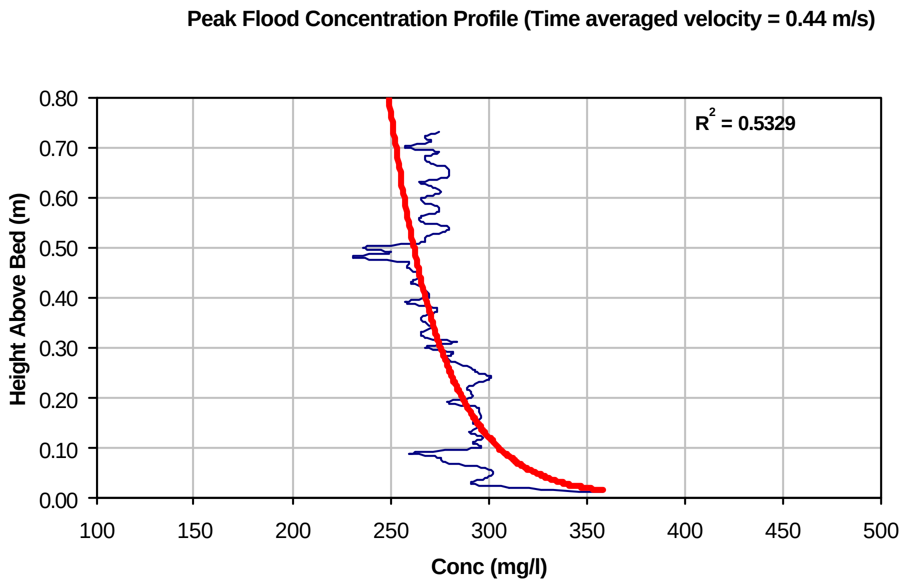

Figure 11: Concentration 1m profile for the flood period.

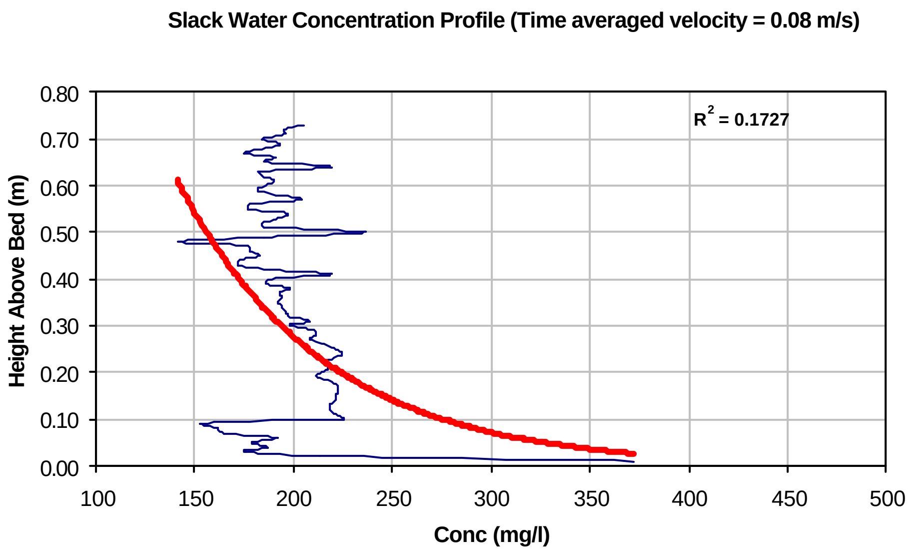

Figure 12: Concentration 1m profile for the slack water period.

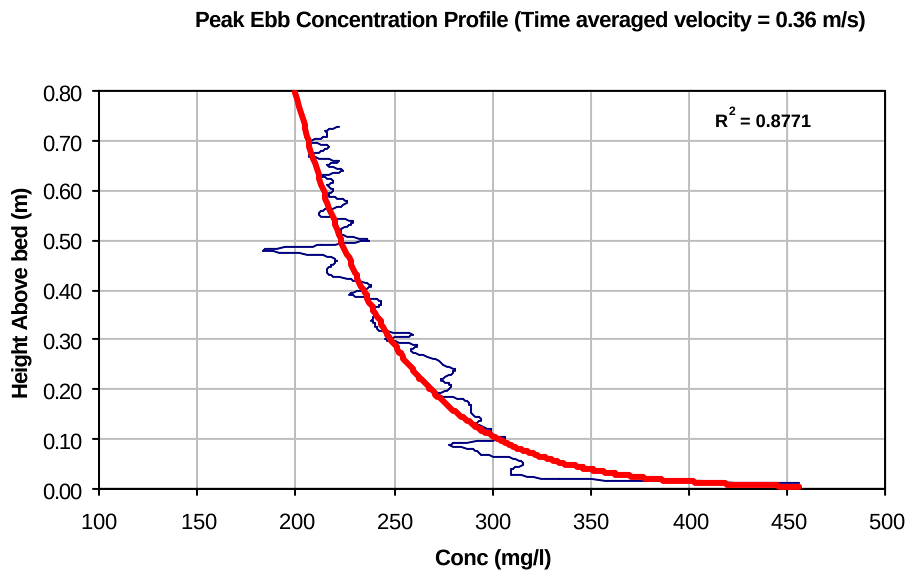

Figure 13: Concentration 1m profile for the ebb period.

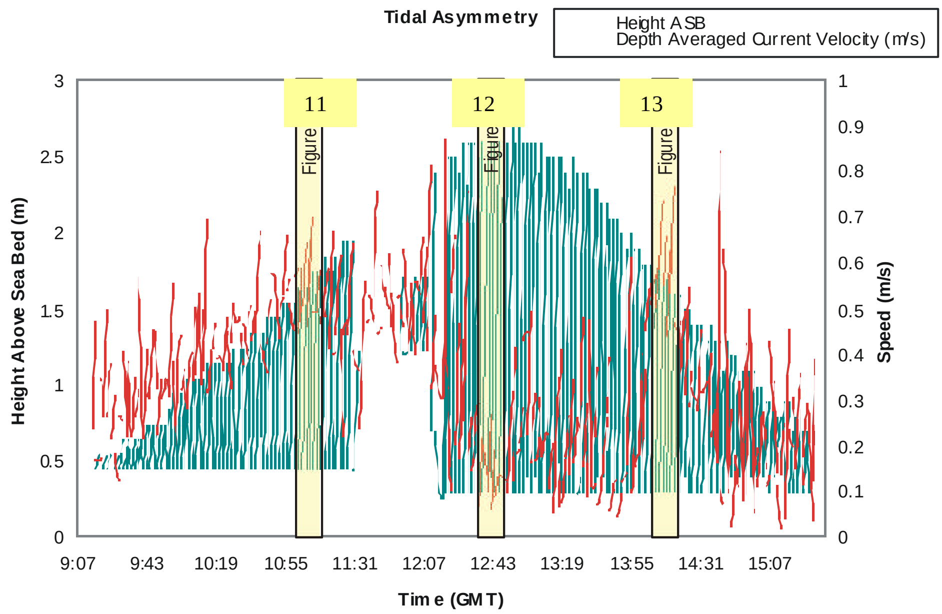

Figure 14: Plot of the tidal asymmetry and depth averaged current speed 1m depth ABS.

All three methods of determining suspended sediment concentrations have produced similar trends throughout the tidal cycle (figure 15), indicating that they have detected variations in concentrations during the same periods. The ASM and pump samples exhibit similar concentration levels, however the LISST has detected a greater range in concentration levels and on average higher concentrations.

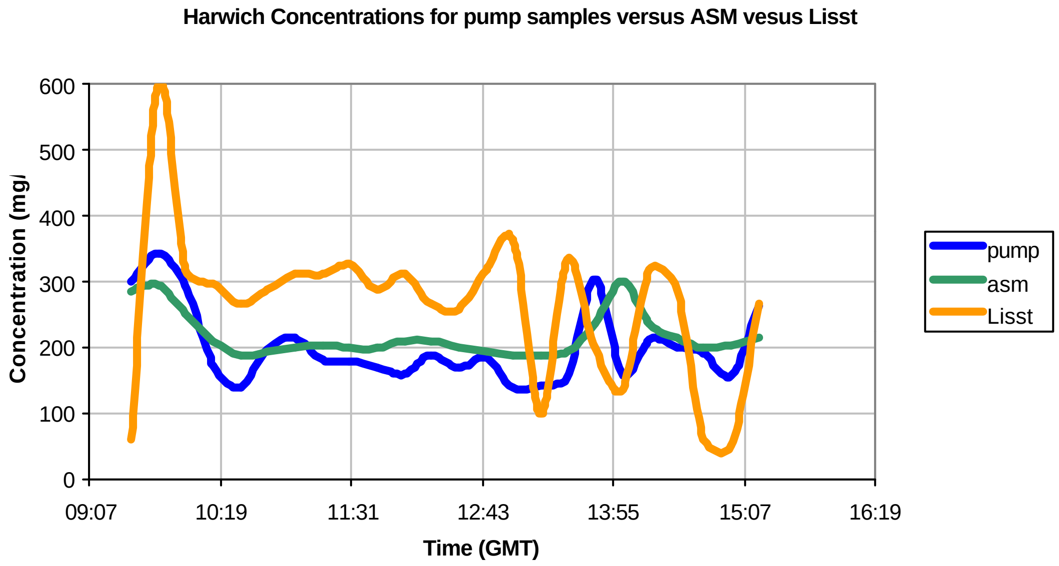

Figure 15: SSC comparisons between bottled pump samples, LISST and Sensor 55 of the ASM (0.2m above the bed). All three methods of determining SSC's have produced similar trends. The ASM and pump samples exhibit similar concentration levels.

3.4 Graphic representation of the total fluxes recorded from the deployment for 1m above the sea bed.

The flux of sediment was calculated once the values of sediment concentration were obtained. Velocity data was obtained using an ADCP, the primary function of which is to record current velocities through the water column. The velocity data and the calculated sediment concentrations were correlated to have the same spatial and temporal resolutions. This allowed a comparison between the amount of sediment at a given depth and time and the speed and direction in which it is travelling. Integrating the product of these over the depth of the water column produces a time series of the sediment flux. Integrating a second time, this time with respect to time, over the duration of the tidal sequence gives the mass of sediment transported per unit width (figure 16).

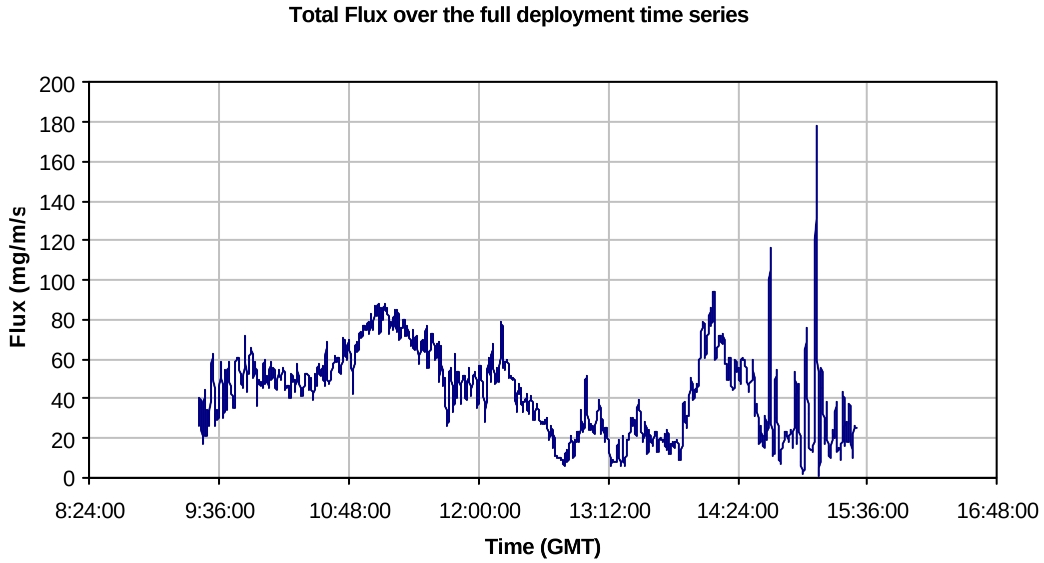

Figure 16: Total flux for full time series, the velocity profiles and SSC profiles were correlated to have the same spatial and temporal resolutions.

4. Conclusion

The aim of the experiment was achieved inasmuch that measurements of the spatial and temporal change in SSC's were obtained over one tidal cycle. The ASM successfully detected a decrease in concentration due to particle settling during the lowest current velocities and re-suspension of particles during peak current flow. Suspended sediment concentration data correlated well with data obtained from the LISST and gravimetrically determined analysis and thus operated favourably as a multi-sensor OBS. The successful integration of the concentration profiles and the velocity profiles enabled the determination of sediment fluxes over one tidal cycle.